

Received: 2017.10.08
Accepted: 2018.04.24
Published: 2018.08.22

ATN-161 as an Integrin $\alpha 5\beta 1$ Antagonist Depresses Ocular Neovascularization by Promoting New Vascular Endothelial Cell Apoptosis

Authors' Contribution:
Study Design A
Data Collection B
Statistical Analysis C
Data Interpretation D
Manuscript Preparation E
Literature Search F
Funds Collection G

ABCDEFG 1 **Ailing Sui**
BCD 1 **Yisheng Zhong**
CEF 2 **Anna M. Demetriades**
CEF 3 **Jikui Shen**
EF 1 **Ting Su**
BCD 1 **Yiyun Yao**
BE 1 **Yushuo Gao**
EF 1 **Yanji Zhu**
AFG 1 **Xi Shen**
AEFG 1 **Bing Xie**

1 Department of Ophthalmology, Ruijin Hospital, Shanghai Jiao Tong University School of Medicine, Shanghai, P.R. China
2 Department of Ophthalmology, New York Presbyterian Hospital-Weill Cornell Medicine, New York, NY, U.S.A.
3 Departments of Ophthalmology and Neuroscience, The Johns Hopkins University School of Medicine, Baltimore, MD, U.S.A.

Corresponding Author: Bing Xie, e-mail: brinkleybing@126.com, Xi Shen: e-mail: carl_shen2005@126.com
Source of support: Supported by the National Natural Science Foundation of China 81470639 and 81570853; Shanghai Natural Science Foundation Grant 14411968400; and 2015 Doctoral Innovation Fund Projects BXJ201414 from Shanghai Jiao Tong University School of Medicine, China

Background: ATN-161 (Ac-PHSCN-NH2), an antagonist of integrin $\alpha 5\beta 1$, has shown an important influence in inhibiting tumor angiogenesis and metastasis of other tumor types. However, the mechanism of action of ATN-161 and whether it can inhibit ocular neovascularization (NV) are unclear. This study investigated the role of ATN-161 in regulating ocular angiogenesis in mouse models and explored the underlying signaling pathway.





Material/Methods: An oxygen-induced retinopathy (OIR) mouse model and a laser-induced choroidal neovascularization (CNV) mouse model were used to test integrin $\alpha 5\beta 1$ expression and the effect of ATN-161 on ocular NV by immunofluorescence staining, Western blot analysis, and flat-mount analysis. The activation of nuclear factor- κ B (NF- κ B), matrix metalloproteinase-2/9 (MMP-2/9), and cell apoptosis were detected by immunofluorescence staining, Western blot, real-time RT-PCR, and terminal deoxynucleotidyl transferase dUTP nick-end labeling (TUNEL). The cell proliferation was detected by BrdU labeling.

Results: In OIR and CNV mice, the protein expression level of integrin $\alpha 5\beta 1$ increased compared with that in age-matched controls. The mice given ATN-161 had significantly reduced retinal neovascularization (RNV) and CNV. Blocking integrin $\alpha 5\beta 1$ by ATN-161 strongly inhibited nuclear factor- κ B (NF- κ B) activation and matrix metalloproteinase-2/9 (MMP-2/9) expression and promoted cell apoptosis, but the effect of ATN-161 on proliferation in CNV mice was indirect and required the inhibition of neovascularization. Inhibiting NF- κ B activation by ammonium pyrrolidinedithiocarbamate (PDT) reduced RNV and promoted cell apoptosis in ocular NV.

Conclusions: Blocking integrin $\alpha 5\beta 1$ by ATN-161 reduced ocular NV by inhibiting MMP-2/MMP-9 expression and promoting the cell apoptosis of ocular NV.

MeSH Keywords: **Apoptosis • Integrin alpha5beta1 • Matrix Metalloproteinases • Neovascularization, Pathologic • NF-kappa B**

Full-text PDF: <https://www.medscimonit.com/abstract/index/idArt/907446>

 3656  —  8  47



Background

Angiogenesis plays a crucial role in physiological and pathological processes such as collateral vessel formation, normal wound repair, arthritis, tumor growth, ischemic retinopathies, and choroidal neovascularization (CNV) [1,2]. The disruption of the balance between anti-angiogenic and pro-angiogenic factors leads to pathological neovascularization (NV). So far, several target molecules related to angiogenesis have been studied and vascular endothelial growth factor (VEGF) was deemed to play a significant role in ocular NV diseases. Anti-VEGF treatment was used to inhibit ocular NV and tumor NV. However, this treatment is effective in only some patients with ocular NV [3,4], and problems such as ocular inflammation [5–7], cardiovascular toxicities [7], ocular hemorrhage, and stroke [8] still need to be resolved. Therefore, potential therapeutic targets in addition to VEGF need to be developed [9].

Integrins are a family of enzymatically inactive cell adhesion receptors, including 19 different α subunits and 8 different β subunits, forming at least 25 different integrins with distinct ligand-binding specificities [10]. Integrin $\alpha 5\beta 1$, as a member of the integrin family, plays a significant role in both cell-cell and cell-extracellular matrix interactions. It also modulates cell adhesion, migration, differentiation, and angiogenesis [10–12]. Integrin $\alpha 5\beta 1$ is a specific receptor of fibronectin and is upregulated in growth factor-induced NV [11,13], whereas the expression of integrin $\alpha 5\beta 1$ is low in quiescent vascular cells [13,14].

ATN-161 is an antagonist of integrin $\alpha 5\beta 1$ derived from the synergy domain (PHSRN) of human fibronectin, in which a cysteine residue takes over from an arginine in the primeval sequence (PHSCN) [15]. Some studies indicated that ATN-161 inhibited tumor growth, metastasis, and extended survival in several tumor models, both as a single agent and in combination with radiochemotherapy [16–18]. Although the importance of ATN-161 in inhibiting tumor angiogenesis and metastasis of other tumor types has been described previously, its mechanism of action and whether ATN-161 inhibits ocular NV is not clear. Therefore, this study investigated the influence of ATN-161 in regulating ocular angiogenesis in mouse models and explored the underlying signaling pathway.

Material and Methods

Animal care and ethics statement

All the mice included in this study were specific pathogen-free and were based on C57BL/6 mice (Charles River, Wilmington, MA). Animal care and all procedures were carried out in accordance with the Health Guide for Care and Use of Laboratory Animals (National Institutes) and were approved

by the Scientific Investigation Board (approval no. SYXK-2003-0026) of Shanghai Jiao Tong University School of Medicine, Shanghai, China.

Mouse model of oxygen-induced retinal neovascularization (RNV) and flat-mount analysis

Seven-day-old C57BL/6 mice were exposed to oxygen ($75\pm 3\%$) for 5 days along with their wet nurse, and were returned to room air at postnatal day 12 (P12), as previously described [19]. At P12, these C57BL/6 mice were randomly divided into groups. Both eyes received an intravitreal injection of 1 μ L of 0.1 μ g/ μ L, 1.0 μ g/ μ L, and 10 μ g/ μ L ATN-161 or 1 μ L of PBS. Pulled glass micropipettes, the Harvard Pump Microinjection System, and a dissecting microscope were used in the course of intraocular injection, as previously described [1]. At P18, the eyes were harvested and fixed in 4% paraformaldehyde solution for at least 4 h at room temperature. Retinas were carefully dissected and incubated with fluorescein isothiocyanate (FITC)-*Griffonia simplicifolia* Lectin-B4 (Vector Laboratories, Inc., CA, USA) for 40 min in the absence of light [4]. After that, the retinas were mounted in fluorescence mounting medium (Dako, Glostrup, Denmark) on glass slides. Retinal flat-mount images were captured under a fluorescence microscope (Nikon, New York, NY) and analyzed using Image-Pro Plus software (Media Cybernetics, Silver Spring, MD, USA).

Mouse model of CNV and flat-mount analysis

CNV was stimulated through laser-induced Bruch's membrane rupture, as described previously [20]. In brief, the pupils from 6- to 8-week-old female mice (C57BL/6) were dilated with 1% tropicamide after being anesthetized with ketamine hydrochloride. Using an OcuLight GL diode laser (Iridex, CA, USA), the laser spots with a bubble without hemorrhage, indicating disrupted Bruch's membranes, were produced, confirmed effective, and then included in the study. The laser parameters were: spot size 100 μ m, 0.1 s duration, and 120 mW. At days 0 (D0) and 7 (D7) after laser treatment, the mice were administered PBS (1 μ L) in one eye and ATN-161 (1 μ L, 1.0 μ g/ μ L) in the other eye. At day 14 (D14), the choroidal membranes of the mice were carefully dissected and flat-mounted after perfusion with 50 mg/mL of fluorescein-labeled dextran (Sigma-Aldrich, MO, USA) from the left ventricle [21], and then photographed using a fluorescence microscope (Nikon, New York, NY). The total area of CNV at each rupture site was assessed using Image-Pro Plus software [21].

Immunofluorescence staining

We prepared 10- μ m-thick slices from eyes of OIR mice, CNV mice, and age-matched controls, fixed them with 4% paraformaldehyde at room temperature, and then permeabilized

them in 0.5% TritonX-100. After blocking in 5% bovine serum albumin, these slices were incubated with integrin $\alpha 5$, integrin $\beta 1$ (Santa Cruz Biotechnology), $\text{I}\kappa\text{B}\alpha$, phosphorylated- $\text{I}\kappa\text{B}\alpha$ (Abcam), p65, and phosphorylated (ser311) p65 (Cell Signaling Technology) primary antibodies overnight, and then incubated in the mixture of FITC-secondary antibodies (Cell Signaling Technology) and Dylight 594 *Griffonia simplicifolia* Lectin-B4 (Vector Laboratories, Inc., CA, USA). Prolong gold antifade reagent with 4', 6-diamidino-2-phenylindole (DAPI) (Invitrogen) was used to incubate the slices before the images of sections were examined and acquired by fluorescence microscopy.

Western blotting

Proteins of retinas harvested from OIR mice at P15 or P18, posterior segments (retina/choroid complex) from CNV mice at D3 or D14, and age-matched controls were extracted using a protein extraction kit (Beyotime, Shanghai, China). Protein concentrations were measured by use of a Bicinchoninic Acid Protein Quantification Assay Kit (Thermo-Fisher Scientific, Göteborg, Sweden). The samples were adjusted into 40- μg protein content and mixed with a suitable volume of 5 \times sodium dodecyl sulfate (SDS)-sample buffer (Thermo-Fisher Scientific), separated in proper SDS gel, and transferred onto polyvinylidene fluoride membranes (Millipore, Bedford, MA, USA). We used 5% nonfat dried milk in Tris-buffered saline (TBS) with Tween 20 (20mM Tris, 100mM NaCl, Ph 7.6, 0.1% Tween 20) to block these membranes. After incubation with primary antibodies overnight at 4°C, membranes were incubated with secondary antibodies conjugated with horseradish peroxidase (Cell Signaling Technology) for 2 h at room temperature. Primary antibodies included integrin $\alpha 5$, integrin $\beta 1$, p65, phosphorylated (ser311) p65, cleaved-poly-ADP-ribose polymerase (PARP), β -actin (Cell Signaling Technology), $\text{I}\kappa\text{B}\alpha$, phosphorylated $\text{I}\kappa\text{B}\alpha$, matrix metalloproteinase-2 (MMP-2), MMP-9 (Abcam), and cleaved caspase-3 (Millipore). Western blotting detection solutions (enhanced chemiluminescence, Millipore) were used to visualize immunoreactive bands, and image J software (National Institutes of Health, MD, USA) was used to measure mean band intensities.

Quantitative reverse transcription polymerase chain reaction (RT-PCR)

Total RNA of retinas from OIR mice and age-matched controls was isolated, and 2 μg of RNA of each sample was reverse-transcribed into complementary DNA (cDNA) using a cDNA synthesis kit (Roche, Basel, Switzerland). RT-PCR was carried out using SYBR Green Mix (Roche, Basel, Switzerland) in a 20 μL volume on the ABI 7500 Real-time PCR system (Applied Biosystems, CA, USA). Housekeeping gene cyclophilin A was used to normalize relative expression of target genes. The relative quantification of different groups was calculated by $2^{-\Delta\Delta\text{CT}}$ method. All PCR primers were as follows:

$\text{I}\kappa\text{B}\alpha$, 5'-AGGACGAGGAGTACGAGCAA-3'(sense), 5'-CGTGGATGATTGCCAAGTGC-3'(antisense); p65, 5'-GCGTACACATTCTGGGGAGT-3'(sense), 5'-ACCGAAGCAGGAGCTATCAA-3'(antisense) [22]; MMP-2, 5'-GCTCTGCTCCTCTGTAGTTA-3'(sense), 5'-GGTACAGTCAGCACCTTTCTT-3'(antisense) [21]; MMP-9, 5'-TGCACTGGGCTTAGATCATT-3'(sense), 5'-TGCCGTCTATGTCGCTTTATTC-3' (antisense) [21]; Cyclophilin A, 5'-CAGACGCCACTGTCGCTTT-3' (sense), 5'-TGCTTTGGAACCTTTGTCTGCAA-3' (antisense) [4].

Terminal deoxynucleotidyl transferase dUTP nick-end labeling (TUNEL)

A mouse model of CNV was established as described earlier. At D0 and D7 after photocoagulation, the mice were given ATN-161 (1 μL , 1 $\mu\text{g}/\mu\text{L}$) or PDTC (1 μL , 10 μM) in one eye and PBS (1 μL) in the other eye. At D14, their eyes were frozen in Tissue-Tek OCT media (Sakura Finetek), and then 10- μm -thick slices were harvested. We used 4% paraformaldehyde to fix tissue sections and permeabilization solution (freshly prepared, 0.1% Trion X-100 in 0.1% sodium citrate) was used to permeabilize the plasma membrane of cells. These sections were then incubated with a terminal deoxynucleotidyl transferase dUTP nick-end labeling (TUNEL) reaction mixture (Roche, Basel, Switzerland) at 37°C for 60 min, Dylight 594 *Griffonia simplicifolia* Lectin-B4 (Vector Laboratories) for 40 min at room temperature, and 4', 6-diamidino-2-phenylindole (DAPI) (Beyotime Biotechnology) for 5 min at room temperature, and then washed for 30 min in PBS. All these procedures were performed in the dark and the surroundings of the samples were kept dry. After mounting the sections with mounting medium (Dako), we used a fluorescence microscope to examine the images.

BrdU labeling and immunofluorescence staining

Proliferation of vascular endothelial cells in CNV mice was assessed by immunofluorescence staining for 5-bromo-2-deoxyuridine (BrdU). At D0 and D7 after photocoagulation, the mice were given an intravitreal injection with ATN-161 (1 μL , 1 $\mu\text{g}/\mu\text{L}$) in one eye and PBS (1 μL) in the other eye. These mice were injected intraperitoneally with BrdU (Sigma, St. Louis, MO) 0.2 mg per gram body weight at D2, D5, D7, D10, D13, and D14 [23,24]. Eyes were collected at D7 and D14 and fixed with 4% paraformaldehyde for 1 h and then cut into 10- μm -thick slices. After being washed and permeabilized in PBS-T (PBS containing 1% Triton X-100) for 30 min, these slices were placed in 2N HCl for 30 min at room temperature and then washed 3 times with PBS-T. Before incubated in the mixture of Alexa 488-conjugated anti-rat secondary antibody (Abcam) and Dylight 594 *Griffonia simplicifolia* Lectin-B4 (Vector Laboratories), the slices were incubated in BrdU primary antibody (Abcam) overnight at 4°C. Prolong gold antifade reagent

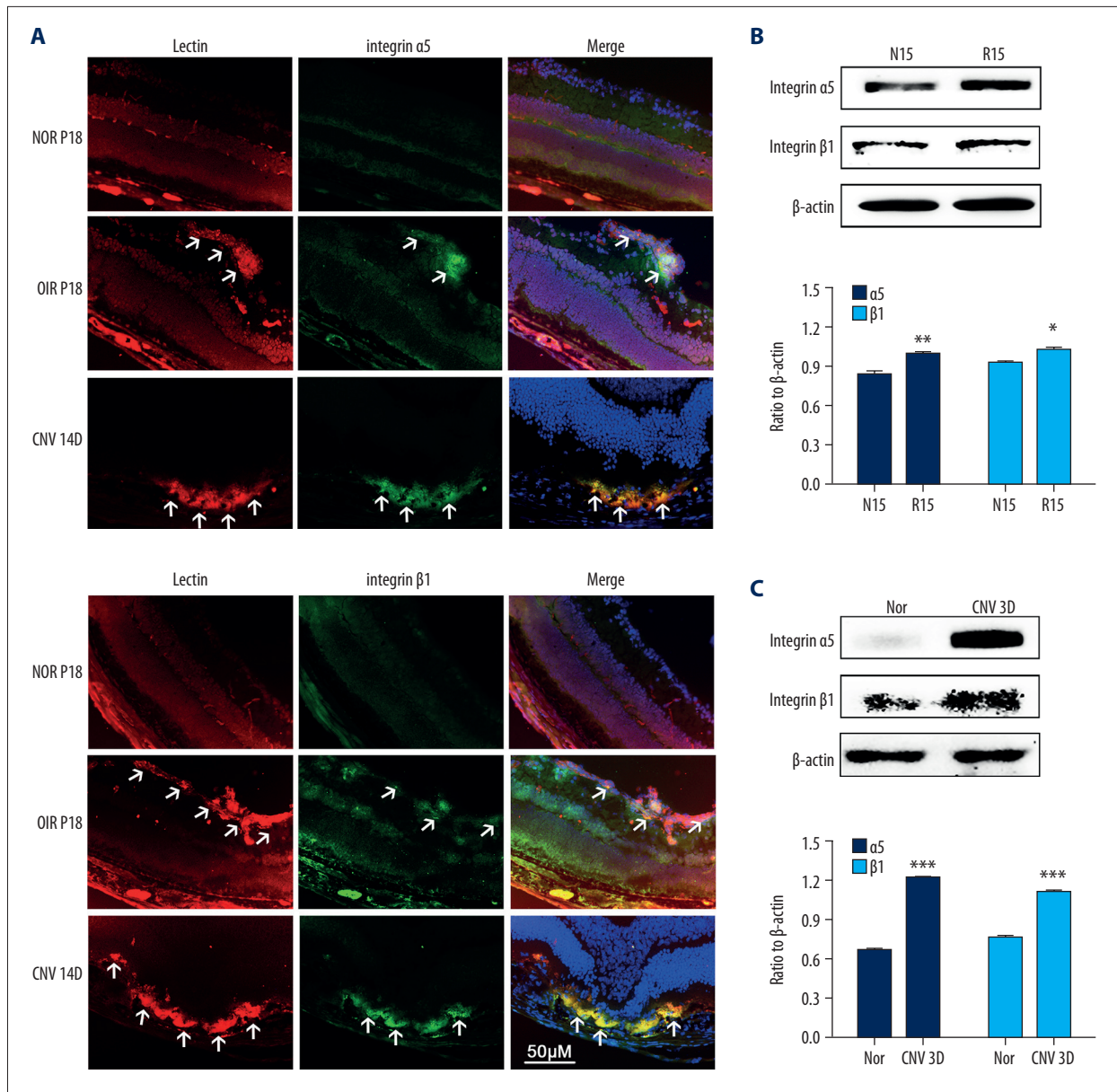


Figure 1. Expression level of integrin $\alpha 5 \beta 1$ in OIR and CNV mice. **(A)** Immunofluorescent staining of integrin $\alpha 5 \beta 1$ and Dylight 594 *Griffonia simplicifolia* Lectin-B4 (a marker for VEC) in OIR, CNV, and age-matched control mice. Arrowheads point to positive areas. **(B, C)** Western blot analysis was used to evaluate integrin $\alpha 5$ and integrin $\beta 1$ expression at P15 in OIR mice on day 3 after photocoagulation in CNV mice and age-matched controls. Relative protein expression of integrin $\alpha 5$ and integrin $\beta 1$ normalized to β -actin. Data are expressed as the mean \pm SEM from 3 independent experiments. Data were analyzed using the *t* test. * $P < 0.05$, ** $P < 0.01$, *** $P < 0.001$.

with DAPI (Invitrogen) was used to label nuclei. The choroidal membranes of the mice were carefully dissected and flat-mounted after performing the steps described above. The images were captured by fluorescence microscopy (Nikon).

Statistical analysis

All data are presented as mean values \pm standard error of the mean (SEM). The two-tailed *t* test was adopted to analyze the differences between 2 groups. The Student-Newman-Keuls method was used to analyze the multiple comparisons. All statistical analyses were performed using SAS 9.0 software (SAS

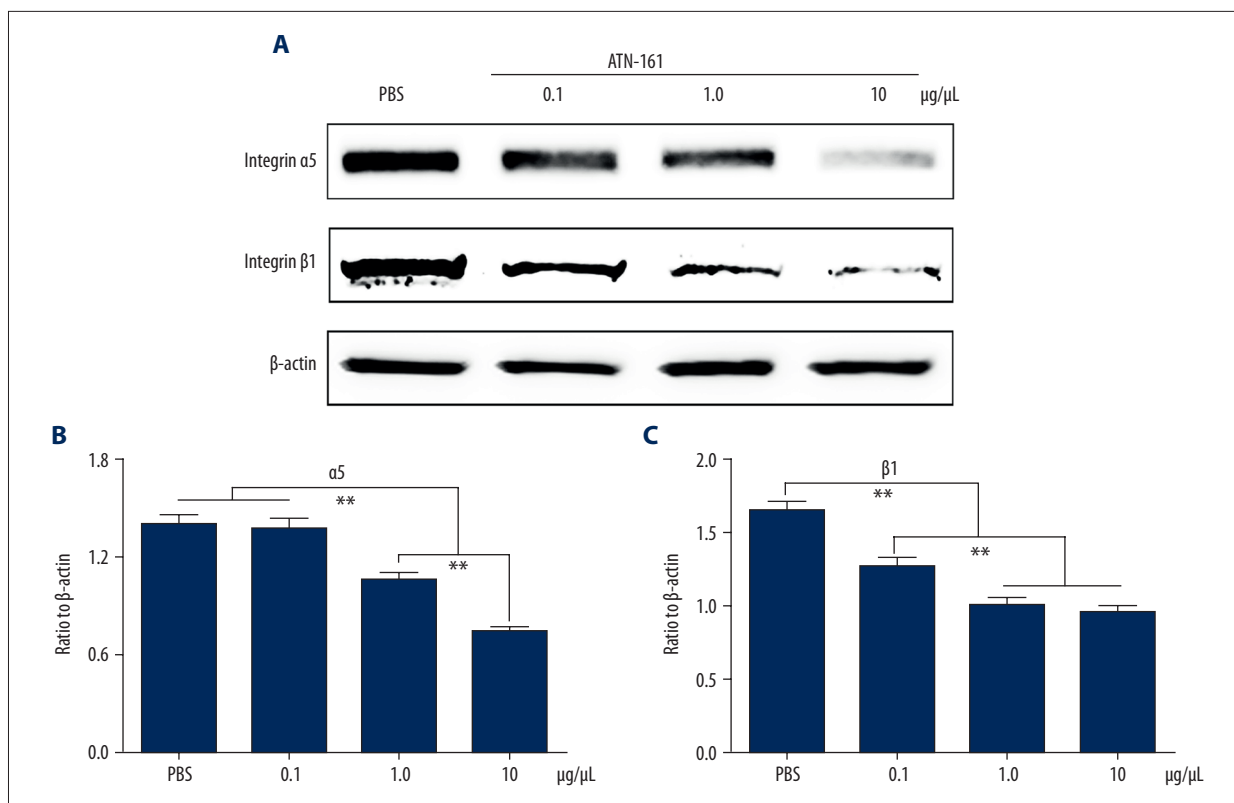


Figure 2. Effect of ATN-161 on integrin $\alpha 5\beta 1$ expression in retinas of OIR mice. OIR model was established as described above. At P12, mice were randomly divided into 4 groups ($n=3$ for each group) and were given an intravitreal injection in both eyes consisting of 1 μL of PBS or 1 μL of different concentrations of ATN-161 (0.1 $\mu\text{g}/\mu\text{L}$, 1.0 $\mu\text{g}/\mu\text{L}$, and 10 $\mu\text{g}/\mu\text{L}$). At P15, retinal protein was isolated. **(A)** Western blot assay images of integrin $\alpha 5\beta 1$. **(B, C)** Graph showing the relative integrin $\alpha 5$ and $\beta 1$ protein levels normalized to β -actin. Mean \pm SEM (from 3 independent experiments) is used to display the results. Data were analyzed by Student-Newman-Keuls method. ** $P<0.01$.

Institute Inc., Cary, NC, USA). $P<0.05$ was considered to be statistically significant.

Results

Expression of integrin $\alpha 5\beta 1$ was increased in retinas of OIR mice and retina/choroid complex of CNV mice

Integrin $\alpha 5\beta 1$ expression in different mouse models (OIR and CNV) was investigated by immunofluorescence staining and Western blot. The protein levels of integrin $\alpha 5$ and $\beta 1$ increased significantly in P15 retinas with OIR and D3 retina/choroid complex with CNV compared with age-matched controls (Figure 1B, 1C). The results of immunofluorescence staining showed that integrin $\alpha 5$ and $\beta 1$ expression levels in OIR and CNV mice were even higher, and the merged images showed that integrin $\alpha 5$ and $\beta 1$ were co-located with vascular endothelial cells (VECs) (Figure 1A). These findings suggest that integrin $\alpha 5\beta 1$ participates in NV progression.

ATN-161 inhibited the expression of integrin $\alpha 5\beta 1$ in retinas of the OIR mice

To investigate the effects and effective concentration of ATN-161, assays were performed in the mouse model of OIR. Western blot assay (Figure 2) demonstrated that ATN-161 significantly inhibited the expression of integrin $\alpha 5\beta 1$ at the concentrations of 1.0 $\mu\text{g}/\mu\text{L}$ and 10 $\mu\text{g}/\mu\text{L}$ compared with PBS-injected eyes.

Intravitreal injection of ATN-161 suppressed the growth of RNV and CNV

The mouse model of OIR was established as described above. Compared with the eyes treated with PBS (Figure 3A), the RNV areas were significantly reduced in eyes treated with 0.1 $\mu\text{g}/\mu\text{L}$ (Figure 3B), 1.0 $\mu\text{g}/\mu\text{L}$ (Figure 3C), and 10 $\mu\text{g}/\mu\text{L}$ (Figure 3D) of ATN-161 ($P<0.05$), which were not significantly different ($P>0.05$, Student-Newman-Keuls, Figure 3E). These findings demonstrate that ATN-161 inhibited RNV in the mouse model of OIR. Based on the results from Figure 2

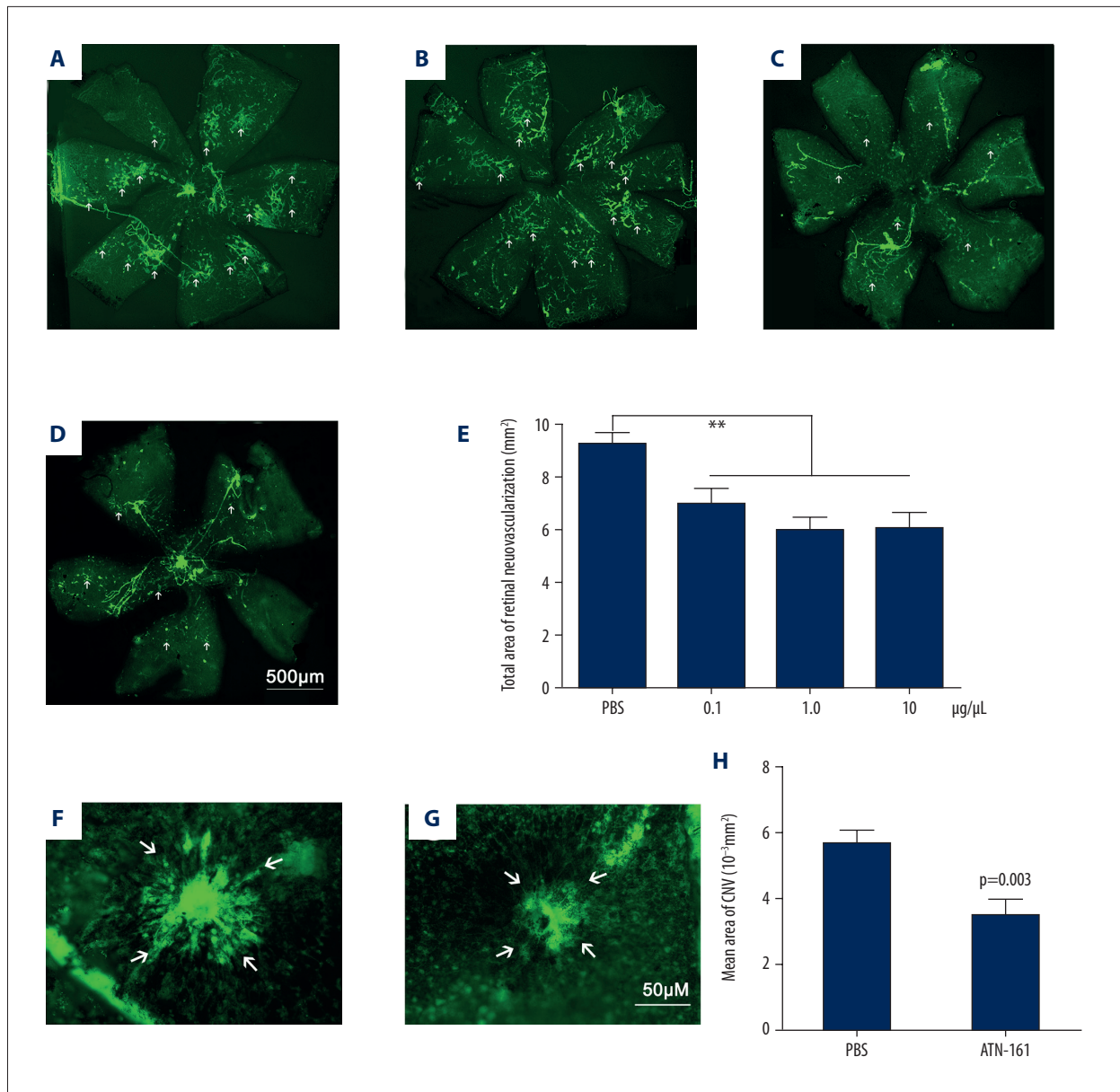


Figure 3. Visualization of the inhibitory effect of ATN-161 on RNV and laser-induced CNV. The mouse model of OIR was established as described above. At P12, the mice were injected intravitreally with PBS (1 μL , **A**, n=11) or ATN-161 at different concentrations (1 μL , **B**: 0.1 $\mu\text{g}/\mu\text{L}$, n=10; **C**: 1.0 $\mu\text{g}/\mu\text{L}$, n=10; **D**: 10 $\mu\text{g}/\mu\text{L}$, n=9) in both eyes. At P18, whole retinas were stained with FITC-lectin and then flat-mounted. Statistical analysis was carried out using Student-Newman-Keuls method and results are shown as the mean \pm SEM (**E**). ** $P < 0.01$. We injected 6- to 8-week-old mice (C57BL/6, female) intravitreally with PBS (1 μL , **F**, n=20) in one eye and ATN-161 (1 μL , 1.0 $\mu\text{g}/\mu\text{L}$, **G**, n=20) in the other eye at days 1 and 7 after laser treatment. The choroidal flat mounts were analyzed after 2 weeks (shown in **H**). Statistical analysis was carried out using the *t* test. Data are expressed as the mean \pm SEM.

and Figure 3A–3E, 1.0 $\mu\text{g}/\mu\text{L}$ was used as an optimal dosage to test the influence of ATN-161 on the CNV model. The choroidal flat mounts indicated that the areas of NV treated with ATN-161 (Figure 3G) were significantly smaller compared with the regions treated with PBS (Figure 3F).

Inhibition of integrin $\alpha 1 \beta 5$ by ATN-161 reduced NF- κ B activation and expression of MMP-2/MMP-9 in OIR mice

The OIR mice were injected intravitreally with different concentrations of ATN-161 (0.1 $\mu\text{g}/\mu\text{L}$, 1.0 $\mu\text{g}/\mu\text{L}$, and 10 $\mu\text{g}/\mu\text{L}$) in one eye and PBS in the other eye at P12. Immunofluorescence

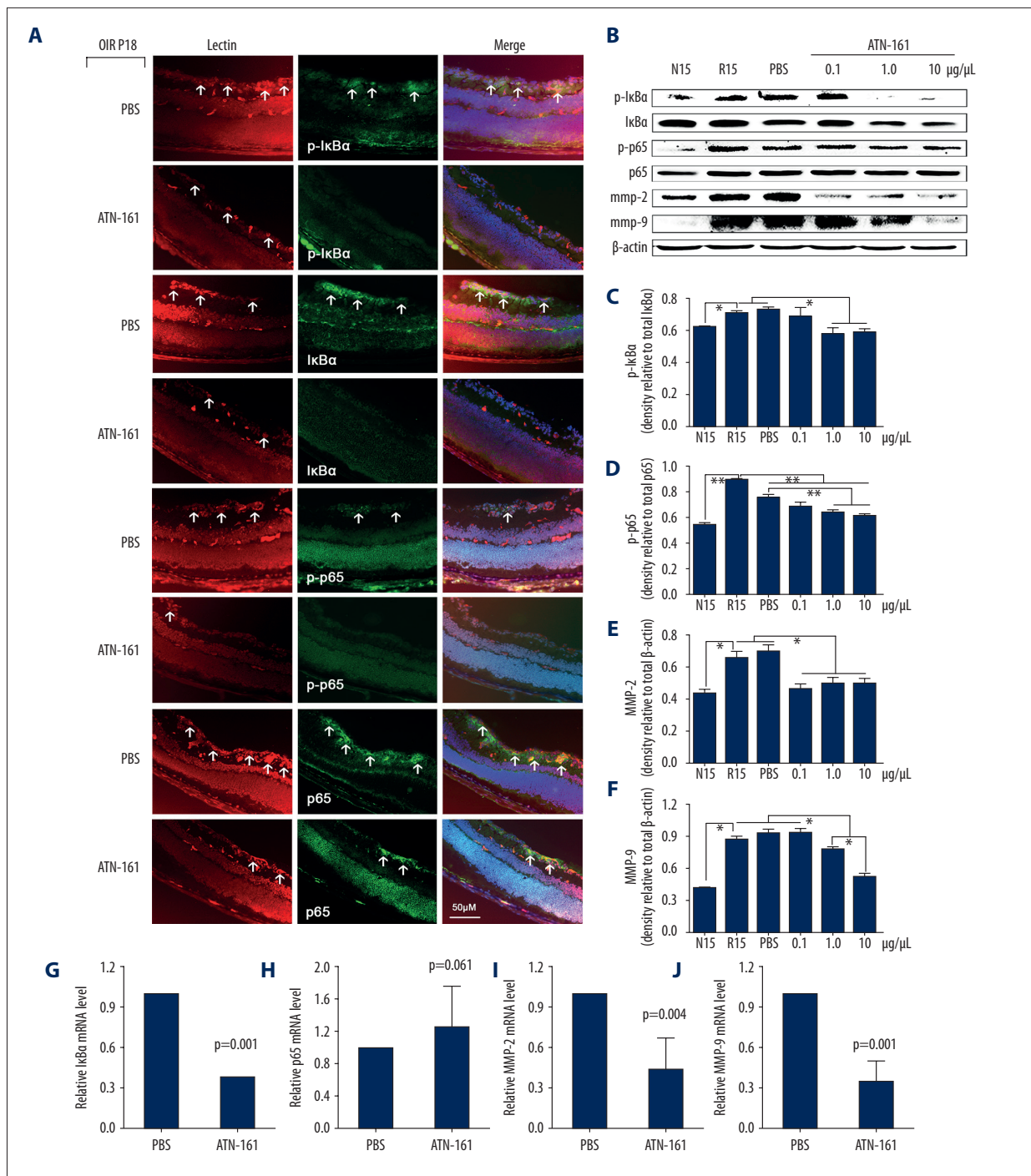


Figure 4. Inhibition of integrin $\alpha 5 \beta 1$ reduced NF- κ B activation and MMP-2/MMP-9 expression in OIR mice. OIR mice were injected intravitreally with 1 μL of PBS or ATN-161 (0.1 $\mu\text{g}/\mu\text{L}$, 1.0 $\mu\text{g}/\mu\text{L}$, and 10 $\mu\text{g}/\mu\text{L}$) at P12. **(A)** Immunofluorescent staining of phosphorylated $\text{IkB}\alpha$ (p-IkBa), total $\text{IkB}\alpha$, phosphorylated p65 (p-p65), total p65, and lectin (red) in OIR mice treated with ATN-161 (1.0 $\mu\text{g}/\mu\text{L}$) or PBS. The arrowheads indicate the positive regions for each labeling staining. **(B)** The retinal proteins of P15 mice were tested by Western blot assays for p-IkBa, total $\text{IkB}\alpha$, p-p65, total p65, MMP-2, MMP-9, and β -actin. **(C-F)** Quantitative assessment of data in B ($n=3$). Three independent assays were performed, and data are shown as the mean \pm SEM. * $P<0.05$, ** $P<0.01$. **(G-J)** OIR mice were injected intravitreally with 1 μL of PBS or 1 μL of ATN-161 (1.0 $\mu\text{g}/\mu\text{L}$) at P12; the retinal mRNA expression levels of $\text{IkB}\alpha$ (**G**, $n=6$), p65 (**H**, $n=6$), MMP-2 (**I**, $n=6$), and MMP-9 (**J**, $n=7$) at P15 were tested by RT-PCR. The $2^{-\Delta\Delta\text{CT}}$ method was used and cyclophilin A was used as endogenous normalization. Statistical analysis was carried out using the t test. Data are expressed as the mean \pm SEM.

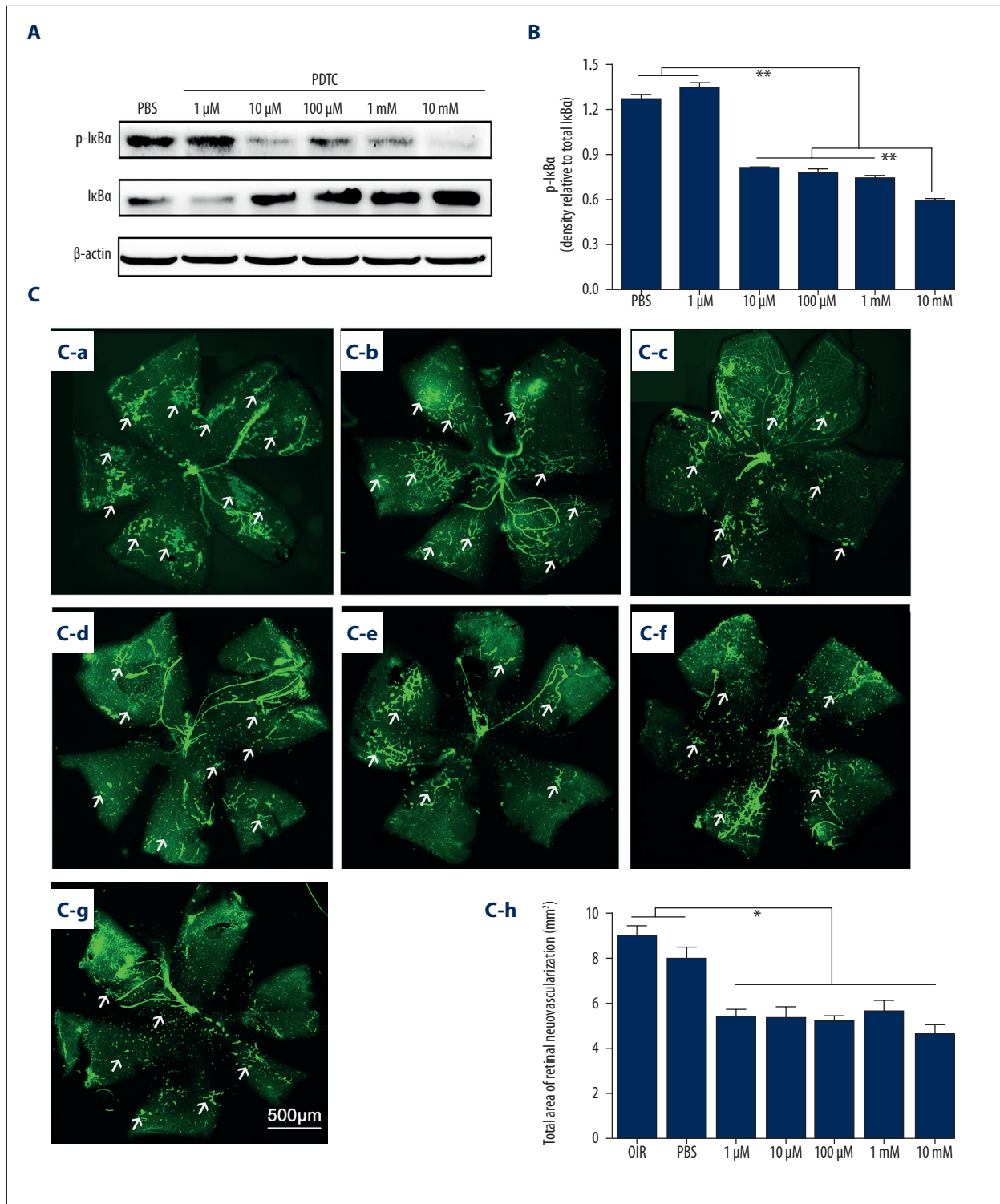


Figure 5. Inhibition of activation of NF- κ B through PDTC reduced RNV in OIR mice. **(A)** At P12, OIR mice were intravitreally injected with 1 μ L of PBS or PDTC (1 μ M, 10 μ M, 100 μ M, 1 mM, and 10 mM). At P15, the retinal total proteins were isolated and determined by Western blot assays for p-I κ B α , total I κ B α , and β -actin. **(B)** Data in A are shown as mean \pm SEM. Student-Newman-Keuls was used for statistical analysis (** $P < 0.01$). **(C)** Whole retinas were stained with FITC-lectin and flat-mounted at P18 **(C-a)**: OIR, n=14; **(C-b)**: PBS, n=14; **(C-c)**: 1 μ M, n=14; **(C-d)**: 10 μ M, n=14; **(C-e)**: 100 μ M, n=14; **(C-f)**: 1 mM, n=14; **(C-g)**: 10 mM, n=14). Statistical analysis was performed using the t test **(C-h)** * $P < 0.05$.

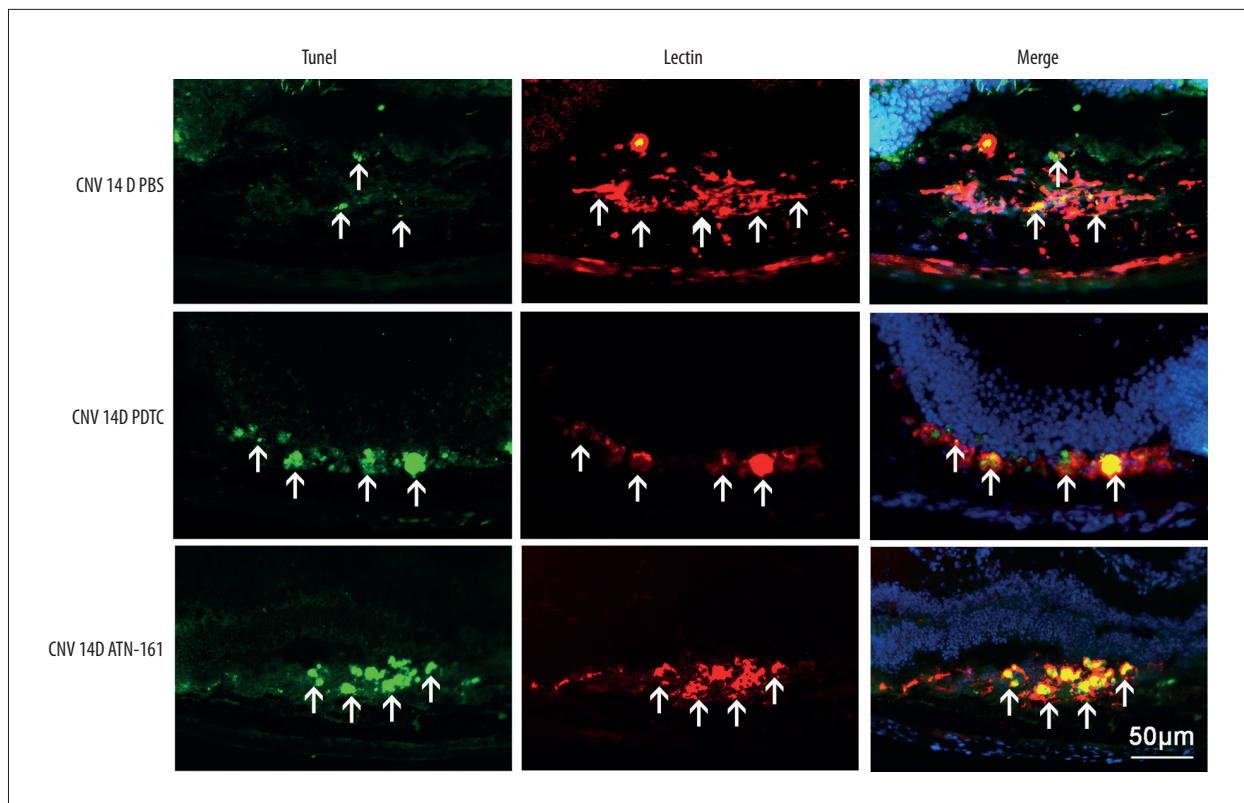


Figure 6. ATN-161 promoted apoptosis in CNV mice. TUNEL staining of murine eyes injected intravitreally with PBS, PDTC (10 μM), or ATN-161 (1.0 $\mu\text{g}/\mu\text{L}$). We injected 6- to 8-week-old mice (C57BL/6, female) intravitreally with 1 μL of PBS in one eye and either 1 μL of ATN-161 (1.0 $\mu\text{g}/\mu\text{L}$) or 1 μL of PDTC (10 μM) in the other eye at days 1 (D1) and 7 (D7) after photocoagulation in CNV mice. At D14, eyes were harvested and 10- μm -thick slices were prepared. These 10- μm -thick slices were double-stained with TUNEL (green) and lectin (red). In the control eyes (treated with PBS), few TUNEL-positive cells were found. However, after intravitreal injection of PDTC or ATN-161, numerous TUNEL-positive cells were observed in CNV eyes. Arrowheads denote the positive area for each labeling staining.

staining in OIR mice at P18 showed that p-I κ B α , I κ B α , p-p65, and p65 were mostly co-located with RNV and the increased expression of p-I κ B α , I κ B α , p-p65, and p65 in OIR mice treated with PBS was significantly inhibited in the OIR mice treated with ATN-161 (Figure 4A). Protein expression of p-I κ B α , I κ B α , p-p65, p65, MMP-2, and MMP-9 from OIR mice at P15 was detected by Western blot assay (Figure 4B). The results revealed that ATN-161 inhibited the activation of NF- κ B (Figure 4C, 4D) and the expression of MMP-2 (Figure 4E) and MMP-9 (Figure 4F). The concentration of 1.0 $\mu\text{g}/\mu\text{L}$ was selected to detect the expression of I κ B α (Figure 4G), p65 (Figure 4H), MMP-2 (Figure 4I), and MMP-9 (Figure 4J) at the RNA level in OIR mice at P15. The results of RT-PCR were similar to the results of Western blot analysis.

Inhibition of NF- κ B activation by PDTC reduced RNV in OIR mice

The OIR mice received intravitreal injections of different concentrations of PDTC in one eye and PBS in the contralateral eye

at P12. Western blot analysis (Figure 5A) was used to evaluate p-I κ B α and I κ B α protein expression at P15. The analysis of results revealed that PDTC significantly reduced the activation of NF- κ B (Figure 5B) at concentrations of 10 μM , 100 μM , 1 mM, and 10 mM. The OIR mice injected intravitreally with PDTC in the eyes appeared to have less RNV compared with the fellow eyes treated with PBS as control (Figure 5C).

ATN-161 and PDTC promoted endothelial cell apoptosis of RNV and CNV

The mice with CNV or OIR were injected intravitreally with 1 μL ATN-161 (1 $\mu\text{g}/\mu\text{L}$) or PDTC (10 μM) in one eye and 1 μL of PBS in the other eye at D0 and D7 (CNV mice) or P12 (OIR mice). The eyes from CNV mice at D14 after photocoagulation and OIR mice at P18 were prepared for TUNEL and Western blot analysis. Observation under a fluorescence microscope revealed that the eyes injected intravitreally with ATN-161 or PDTC had less NV and more TUNEL-positive cells compared with controls in both models (Figure 6). The Western blot assays showed

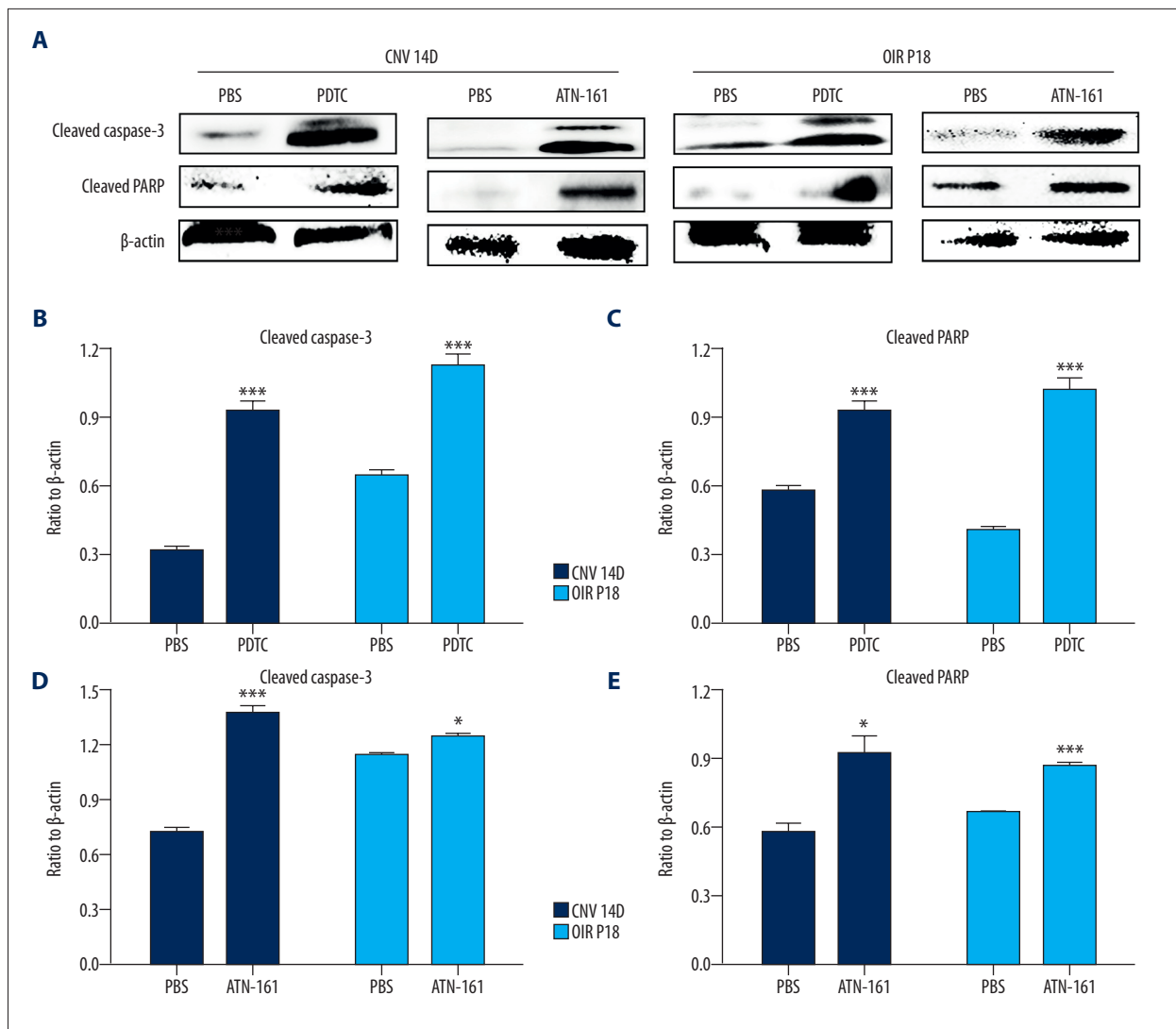


Figure 7. Protein expression levels of cleaved caspase-3 and cleaved PARP in CNV and OIR mice. Western blot assays were used to evaluate protein expression levels of cleaved caspase-3 and cleaved PARP in OIR and CNV mice treated with PDTC (10 μ M), ATN-161 (1 μ g/ μ L) or PBS. Statistical analysis of cleaved caspase-3 and PARP is shown above. Data are expressed as mean \pm SEM. Statistical analysis performed using the *t* test. * $P < 0.05$, ** $P < 0.01$, *** $P < 0.001$.

that ATN-161 and PDTC promoted the cleavage of caspase-3 and PARP (Figure 7). All of these data show that ATN-161 promoted endothelial cell apoptosis of RNV and CNV.

Effect of ATN-161 on CNV and cell proliferation *in vivo*

To assess the effect of ATN-161 to vascular cell proliferation *in vivo*, we evaluated the BrdU labeling in CNV mice at D7 and D14. The immunofluorescence staining analysis of CNV mice treated with PBS or ATN-161 (1 μ g/ μ L) showed that CNV- and BrdU-positive cells significantly decreased following treatments with ATN-161, while the ratio of BrdU- and CD31-positive cells (BrdU/CD31) was not significantly different between the 2 groups (PBS group and ATN-161 group) (Figure 8).

All these results indicate that the effects of ATN-161 on proliferation in CNV mice were indirect and needed the inhibition of neovascularization.

Discussion

The aim of our study was to determine the influence of ATN-161 in ocular NV and to explore the underlying mechanisms. The roles of integrin $\alpha 5\beta 1$ in angiogenesis have been well studied in tumor research. Research showed that integrin $\alpha 5\beta 1$ was upregulated in tumor angiogenesis, but not in normal vasculature [13]. In early atherogenesis, integrin $\alpha 5\beta 1$ signaling critically regulated oxLDL-induced pro-inflammatory responses [25].

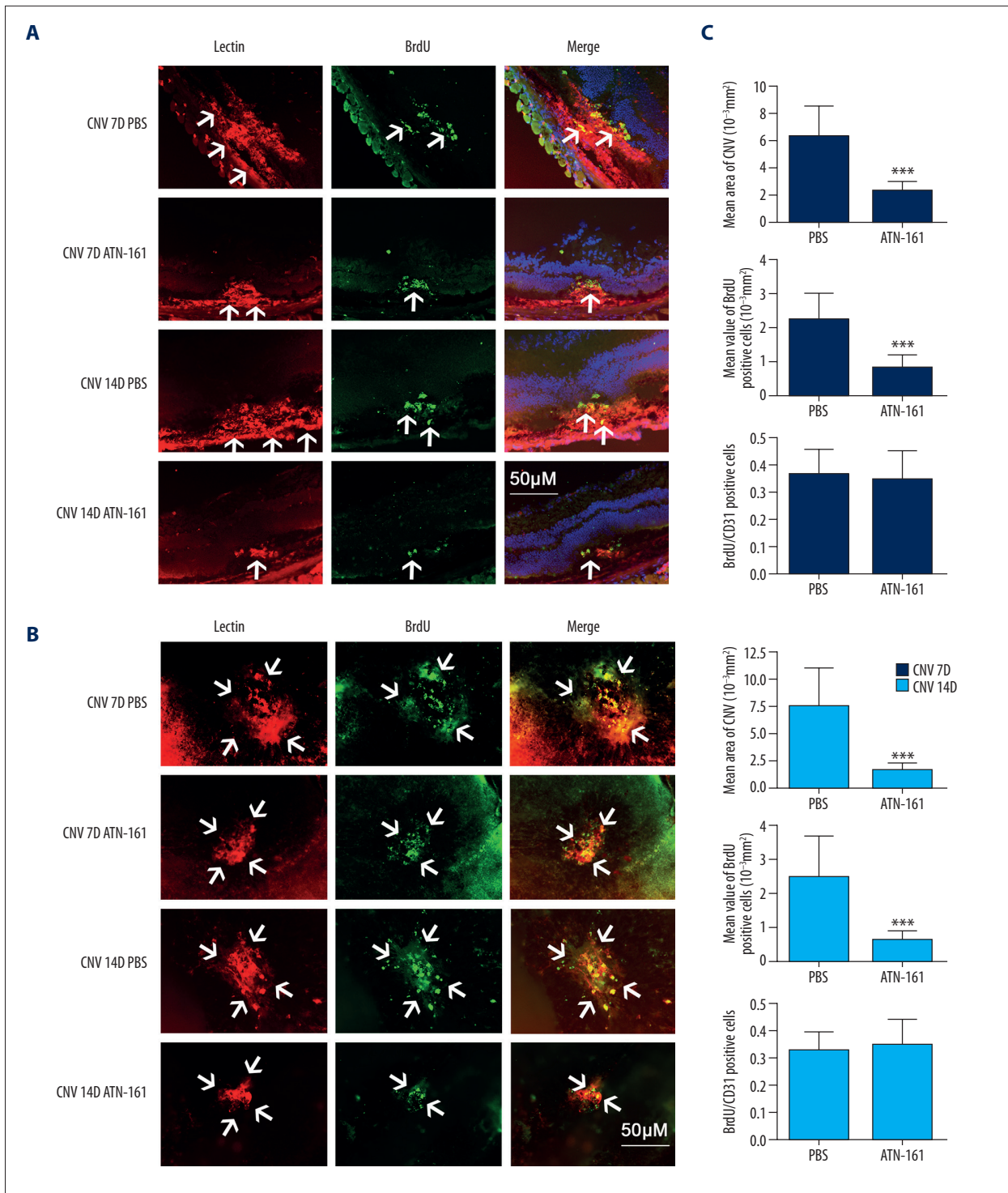


Figure 8. Effect of ATN-161 on NV and cell proliferation in CNV mice. The CNV mice were labeled with BrdU at D2, D5, D7, D10, D13, and D14 by intraperitoneal injection and treated with ATN-161 (1.0 $\mu\text{g}/\mu\text{L}$) or PBS at D0 and D7 by intravitreal injection. **(A)** Immunofluorescent staining of lectin and BrdU from CNV mice treated with ATN-161 (1.0 $\mu\text{g}/\mu\text{L}$) or PBS. **(B)** Immunofluorescent images of flat-mounted choroids from CNV mice at D7 and D14. The arrowheads indicate the positive regions for each labeling staining. **(C)** CNV, BrdU-positive cells, and BrdU/CD31 (the ratio)-positive cells analysis of CNV mice at D7 (PBS group, n=11; ATN-161 group, n=15), D14 (PBS group, n=15; ATN-161 group, n=16). Data were expressed as mean \pm SEM and were analyzed using the *t* test. *** $P < 0.001$.

Some research demonstrated that although ATN-161 could interact with multiple integrin β subunits, it has only been shown to inhibit $\alpha 5\beta 1$ integrin signaling [25]. A phase I clinical trial showed an excellent safety profile for the use of ATN-161 in patients with advanced solid tumors [26]. ATN-161 could also be redirected for use in atherosclerosis [25]. Similar results were obtained with ATN-161 in assays using the models of colon and prostate cancer, which showed antitumor activity as well as the ability to inhibit soft tissue metastasis [17,18]. However, few studies investigated ocular NV. Some research showed that in activated ARPE-19 cells and proliferative vitreoretinopathy membranes, the expression of integrin $\alpha 5\beta 1$ was higher compared with that in the control eyes [27]. In our present study, 2 mouse models of ocular NV were used to investigate the potential role and underlying mechanism of action of ATN-161. The protein levels of integrin $\alpha 5\beta 1$ increased in the CNV and OIR mice, indicating a close relationship between integrin $\alpha 5\beta 1$ and ocular NV. Next, we explored the inhibition of integrin $\alpha 5\beta 1$ by ATN-161 and demonstrated that ATN-161 inhibited the protein expression of integrin $\alpha 5\beta 1$ in a dose-dependent manner. This was similar to the findings of a recent study, which showed that the VEGF-mediated increase in integrin $\alpha 5\beta$ expression was inhibited by ATN-161 [28]. The NV areas were reduced in OIR and CNV mice after treatment with ATN-161 compared with PBS groups. These results further support the important role of integrin $\alpha 5\beta 1$ in NV and extend the findings of a previous study demonstrating that integrin $\alpha 5\beta 1$ is expressed in 2 eyes with proliferative vitreoretinopathy (PVR) [29] but was not expressed in the normal retinal pigment epithelium cell layer [30]. These results are in accordance with a recent study showing that integrin $\alpha 5\beta 1$ participates in the development and progression of CNV, and ATN-161 inhibited laser-induced CNV [28].

The process of angiogenesis is complicated and involves extracellular matrix proteolysis, endothelial cells proliferation and migration, and synthesis of the new matrix in the destination [31]. Because of their ability to degrade basal membrane and extracellular matrix proteins, MMP family proteins play significant roles in angiogenesis. More and more studies demonstrate that MMP-2 and MMP-9 are released at the site of inflammation to regulate angiogenesis [32] and contribute significantly to the development of diabetic retinopathy (DR) [33–35]. In our study, MMP-2 and MMP-9 expression increased in the OIR mice compared with the standard mice. When treated with ATN-161, the MMP-2 and MMP-9 mRNA and protein expression of OIR mice significantly decreased. These data suggest that ATN-161 reduces ocular NV by inhibiting MMP-2 and MMP-9 expression.

NF- κ B is normally sequestered by I κ B in the cytoplasm. I κ B phosphorylation results in ubiquitin-dependent protein degradation, and subsequently releases I κ B-bounded NF- κ B from the

cytoplasm. The entry of NF- κ B to nuclei activates transcription of many cytokines, chemokines, and growth factor genes [36]. NF- κ B is an important therapeutic target in several chronic inflammatory diseases, enabling conspicuous downregulation of macrophage-produced pro-inflammatory cytokines [37–39]. In cancer, NF- κ B activation has been correlated with cell proliferation, survival, invasion, and angiogenesis, making it a potentially desirable target for therapy. Agents that inhibit NF- κ B have been shown to reduce tumor growth and induce apoptosis in malignant cells [40]. Nuclear localization of NF- κ B is associated with breast cancer and may be associated with the escape of these tumor cells from apoptosis [41]. This phenomenon was also observed in cell models [42,43]. All of these results indicate that activation of NF- κ B inhibits apoptosis. In our study, the activation of NF- κ B signaling was increased in OIR mice compared with normal control mice. PDTC was used to block NF- κ B signal activation, and the area of RNV was estimated through flat-mount analysis in the OIR mice treated with PDTC. The assays showed that the area of RNV in the PDTC group was decreased compared with the OIR mice treated with PBS. To further validate the underlying mechanism *in vivo*, assays were performed with different concentrations of ATN-161 to detect the activation of p-I κ B α and p-p65 in the OIR mouse model. The results indicated that ATN-161 decreased the activation of NF- κ B in the OIR mice. The CNV and OIR mice treated with ATN-161 were used to detect the protein levels of cleaved caspase-3 and PARP by Western blot and cell apoptosis by TUNEL. The results indicated that blocking the expression of integrin $\alpha 5\beta 1$ by ATN-161 or the activation of NF- κ B by PDTC induced the cleavage of caspase-3 and PARP, and led to apoptosis.

Reduced neovascularization could be a result of either apoptosis or suspended proliferation, or both. To determine if ATN-161 affects vascular cell proliferation aside from apoptosis, we evaluated the effect of ATN-161 on cell proliferation by BrdU labeling in the CNV mouse model. In previous studies, the expression of integrin $\alpha 5\beta 1$ increased in response to angiogenic factors [28,44] and the interaction between fibronectin and integrin $\alpha 5\beta 1$ has been found to promote cell proliferation in human RPE [27,45], human choroidal endothelial cells (hCECs) [28], and vascular endothelial cells [46]. However, ATN-161 did not attenuate the VEGF-induced proliferation of hCECs at any concentration [28]. Another study of serum-driven MDA-MB-231 cell has shown that ATN-161 did not seem to inhibit cell proliferation *in vitro*. It has been reported that the lack of an anti-proliferative effect of ATN-161 on MDA-MB-231 cells *in vitro* could be explained by low copy numbers of integrin $\alpha 5\beta 1$ and $\alpha v\beta 3$, an alternate receptor for ATN-161, or the insufficient simultaneous inhibition of MAPK and FAK signaling [16,47]. In contrast, ATN-161 had a significant influence on the proliferation of MDA-MB-231 tumors *in vivo*, indicating that the effects of ATN-161 on proliferation *in vivo* were indirect and required the inhibition of angiogenesis [16]. In our study, the

immunofluorescence staining analysis of CNV mice showed that CNV- and BrdU-positive cells significantly decreased following treatments with ATN-161, while the ratio of BrdU- and CD31-positive cells (BrdU/CD31) was not significantly different between the 2 groups (PBS group and ATN-161 group). Our results are consistent with previous research, indicating that reduced neovascularization is a result of promoting apoptosis, not the cause of directly suspended proliferation *in vivo*.

Conclusions

The main findings of our study are: (1) blocking integrin $\alpha 5\beta 1$ through ATN-161 can inhibit ocular NV, suggesting that ATN-161

is a potential treatment for ocular diseases associated with angiogenesis; and (2) Blocking integrin $\alpha 5\beta 1$ strongly inhibited expression of MMP-2/MMP-9 and promoted cell apoptosis of ocular NV. These results suggest a novel therapy for angiogenesis-related ocular diseases aside from anti-VEGF therapy.

Acknowledgment

The authors are grateful for facility and field assistance from the Shanghai Institute of Burns.

Conflict of interest

None.

References:

- Mori K, Duh E, Gehlbach P et al: Pigment epithelium-derived factor inhibits retinal and choroidal neovascularization. *J Cell Physiol*, 2001; 188(2): 253–63
- Campochiaro PA: Ocular neovascularization. *J Mol Med*, 2013; 91(3): 311–21
- Rofagha S, Bhisitkul RB, Boyer DS et al: Seven-year outcomes in ranibizumab-treated patients in anchor, marina, and horizon: A multicenter cohort study (SEVEN-UP). *Ophthalmology*, 2013; 120(11): 2292–99
- Zhu Y, Tan W, Demetriades AM et al: IL-17A neutralization alleviated ocular neovascularization by promoting M2 and mitigating M1 macrophage polarization. *Immunology*, 2015; 147: 414–28
- Kamba T, McDonald DM: Mechanisms of adverse effects of anti-VEGF therapy for cancer. *Br J Cancer*, 2007; 96: 1788–95
- Day S, Acquah K, Mruthyunjaya P et al: Ocular complications after anti-vascular endothelial growth factor therapy in medicare patients with age-related macular degeneration. *Am J Ophthalmol*, 2011; 152(2): 266–72
- Tolentino M: Systemic and ocular safety of intravitreal anti-VEGF therapies for ocular neovascular disease. *Surv Ophthalmol*, 2011; 56(2): 95–113
- Van der Reis MI, La Heij EC, De Jong-Hesse Y et al: A systematic review of the adverse events of intravitreal anti-vascular endothelial growth factor. *Retina*, 2016; 31(8): 1449–69
- Xu Q, Bai Y, Huang L et al: Knockout of a A-Crystallin inhibits ocular neovascularization. *Investig Ophthalmol Vis Sci*, 2015; 56(2): 816–26
- Sørensen BH, Rasmussen LH, Broberg BS et al: Integrin $\beta 1$, osmosensing, and chemoresistance in mouse ehrlich carcinoma cells. *Cell Physiol Biochem*, 2015; 36(1): 111–32
- Hynes RO: Integrins: Bidirectional, allosteric signaling machines. *Cell*, 2002; 110(6): 673–87
- Humphries JD, Byron A, Humphries MJ: Integrin ligands at a glance. *J Cell Sci*, 2006; 119(19): 3901–3
- Kim S, Bell K, Mousa SA, Varner JA: Regulation of angiogenesis *in vivo* by ligation of integrin $\alpha 5\beta 1$ with the central cell-binding domain of fibronectin. *Am J Pathol*, 2000; 156(4): 1345–62
- Okamoto N, Tobe T, Hackett SF et al: Transgenic mice with increased expression of vascular endothelial growth factor in the retina: A new model of intraretinal and subretinal neovascularization. *Am J Pathol*, 1997; 151(1): 281–91
- Parry GC, Shaked Y, Hensley H et al: Pharmacology of the novel antiangiogenic peptide ATN-161 (Ac-PHSCN-NH₂): Observation of a U-shaped dose-response curve in several preclinical models of angiogenesis and tumor growth. *Clin Cancer Res*, 2008; 14(7): 2137–44
- Khalili P, Arakelian A, Chen G et al: A non-RGD-based integrin binding peptide (ATN-161) blocks breast cancer growth and metastasis *in vivo*. *Mol Cancer Ther*, 2006; 5(9): 2271–80
- Stoeltzing O, Liu W, Reinmuth N et al: Inhibition of integrin $\alpha 5\beta 1$ function with a small peptide (ATN-161) plus continuous 5-FU infusion reduces colorectal liver metastases and improves survival in mice. *Int J Cancer*, 2003; 104: 496–503
- Livant DL, Brabec RK, Pienta KJ et al: Anti-invasive, antitumorigenic, and antimetastatic activities of the PHSCN sequence in prostate carcinoma. *Cancer Res*, 2000; 60(2): 309–20
- Shen J, Xie B, Dong A et al: *In vivo* immunostaining demonstrates macrophages associate with growing and regressing vessels. *Invest Ophthalmol Vis Sci*, 2007; 48(9): 4335–41
- Zhu Y, Lu Q, Shen J et al: Improvement and optimization of standards for a preclinical animal test model of laser induced choroidal neovascularization. *PLoS One*, 2014; 9(4): e94743
- Cai Y, Tan W, Shen X et al: Neutralization of IL-23 depresses experimental ocular neovascularization. *Exp Eye Res*, 2016; 146: 242–51
- Kowluru RA, Santos JM, Zhong Q: Sirt1, a negative regulator of matrix metalloproteinase-9 in diabetic retinopathy. *Invest Ophthalmol Vis Sci*, 2014; 55(9): 5653–60
- Wang S, Park S, Fei P et al: Bim is responsible for the inherent sensitivity of the developing retinal vasculature to hyperoxia. *Dev Biol*, 2011; 349(2): 296–309
- Kiyama T, Li H, Gupta M et al: Distinct neurogenic potential in the retinal margin and the pars plana of mammalian eye. *J Neurosci*, 2012; 32(37): 12797–807
- Yurdagül A, Green J, Albert P et al: $\alpha 5\beta 1$ integrin signaling mediates oxidized low-density lipoprotein-induced inflammation and early atherosclerosis. *Arterioscler Thromb Vasc Biol*, 2014; 34(7): 1362–73
- Cianfrocca ME, Kimmel KA, Gallo J et al: Phase 1 trial of the antiangiogenic peptide ATN-161 (Ac-PHSCN-NH₂), a beta integrin antagonist, in patients with solid tumours. *Br J Cancer*, 2006; 94(11): 1621–26
- Zahn G, Volk K, Lewis GP et al: Assessment of the integrin $\alpha 5\beta 1$ antagonist JSM6427 in proliferative vitreoretinopathy using *in vitro* assays and a rabbit model of retinal detachment. *Invest Ophthalmol Vis Sci*, 2010; 51(2): 1028–35
- Wang W, Wang F, Lu F et al: The antiangiogenic effects of integrin $\alpha 5\beta 1$ inhibitor (ATN-161) *in vitro* and *in vivo*. *Invest Ophthalmol Vis Sci*, 2011; 52(10): 7213–20
- Robbins SG, Brem RB, Wilson DJ et al: Immunolocalization of integrins in proliferative retinal membranes. *Invest Ophthalmol Vis Sci*, 1994; 35(9): 3475–85
- Brem RB, Robbins SG, Wilson DJ et al: Immunolocalization of integrins in the human retina. *Invest Ophthalmol Vis Sci*, 1994; 35(9): 3466–74
- Risau W: Mechanisms of angiogenesis. *Nature*, 1997; 386(6626): 671–74
- Schrufer R, Lutze N, Schymeinsky J et al: Human neutrophils promote angiogenesis by a paracrine feedforward mechanism involving endothelial interleukin-8. *Am J Physiol Hear Circ Physiol*, 2005; 288(3): 1186–92
- Gong CY, Yu ZY, Lu B et al: Ethanol extract of dendrobium chrysotoxum lindl ameliorates diabetic retinopathy and its mechanism. *Vascul Pharmacol*, 2014; 62(3): 134–42
- Kowluru RA, Zhong Q, Santos JM: Matrix metalloproteinases in diabetic retinopathy: Potential role of MMP-9. *Expert Opin Investig Drugs*, 2012; 21(6): 797–805

35. Mohammad G, Siddiquei MM: Role of matrix metalloproteinase-2 and -9 in the development of diabetic retinopathy. *J Ocul Biol Dis Inf*, 2012; 5: 1–8
36. Häcker H, Karin M: Regulation and function of IKK and IKK-related kinases. *Sci STKE*, 2006; 375: 1–20
37. Kim HG, Koh GY: Lipopolysaccharide activates matrix metalloproteinase-2 in endothelial cells through an NF- κ B-dependent pathway. *Biochem Biophys Res Commun*, 2000; 269(2): 401–5
38. Joyce D, Albanese C, Steer J et al: NF- κ B and cell-cycle regulation: The cyclin connection. *Cytokine Growth Factor Rev*, 2001; 12(1): 73–90
39. Lee NK, Hwang K, Young S: TNF-related weak inducer of apoptosis receptor, a TNF receptor superfamily member, activates NF- κ B through TNF receptor-associated factors. *Biochem Biophys Res Commun*, 2003; 305: 789–96
40. Brown M, Cohen J, Arun P et al: NF- κ B in carcinoma therapy and prevention. *Expert Opin Ther Targets*, 2009; 12(9): 1109–22
41. Sovak MA, Bellas RE, Kim DW et al: Aberrant nuclear factor- κ B/Rel expression and the pathogenesis of breast cancer. *J Clin Invest*, 1997; 100(12): 2952–60
42. Budunova IV, Perez P, Vaden VR et al: Increased expression of p50-NF- κ B and constitutive activation of NF- κ B transcription factors during mouse skin carcinogenesis. *Oncogene*, 1999; 18: 7423–31
43. Mayo MW, Baldwin AS: The transcription factor NF- κ B, control of oncogenesis and cancer-therapy resistance. *Biochim Biophys Acta*, 2000; 1470(2): 55–62
44. Enaida H, Ito T, Oshima Y et al: Effect of growth factors on expression of integrin subtypes in microvascular endothelial cells isolated from bovine retinas. *Fukushima J Med Sci*, 1998; 44(1): 43–52
45. Li R, Maminishkis A, Zahn G et al: Integrin $\alpha 5\beta 1$ mediates attachment, migration, and proliferation in human retinal pigment epithelium: Relevance for proliferative retinal disease. *Invest Ophthalmol Vis Sci*, 2009; 50(12): 5988–96
46. Wilson SH, Ljubimov AV, Morla AO et al: Fibronectin fragments promote human retinal endothelial cell adhesion and proliferation and ERK activation through $\alpha 5\beta 1$ integrin and PI 3-kinase. *Invest Ophthalmol Vis Sci*, 2003; 44(4): 1704–15
47. Campbell S, Otis M, Cote M et al: Connection between integrins and cell activation in rat adrenal glomerulosa cells: A role for Arg-Gly-Asp peptide in the activation of the p42/p44(mapk) pathway and intracellular calcium. *Endocrinology*, 2003; 144(4): 1486–95